PHYSICAL REVIEW B VOLUME 18, NUMBER 6 15 SEPTEMBER 1978

Electronic energy-band structure of α quartz

Eduardo Calabrese
Sherman Fairchild Laboratory, Lehigh University, Bethlehem, Pennsylvania 18015
and Istituto di Fisica dell' Università, Gruppo Nazionale di Struttura della Materia del C.N.R., 43100 Parma, Italy

W. Beall Fowler
Department of Physics and Sherman Fairchild Laboratory, Lehigh University, Bethlehem, Pennsylvania 18015
(Received 29 June 1977)

The electronic energy bands of silicon dioxide in the α-quartz structure have been calculated at several points of high symmetry in the Brillouin zone by the mixed-basis method. A tight-binding interpolation scheme has been used to determine complete valence bands and their state densities. The results are compared with experiment and with calculations on the higher-symmetry β-cristobalite. The quartz and cristobalite bands share many properties; for example, in both cases the optical-absorption edge is predicted to be direct but forbidden. These results are in partial agreement with pseudopotential calculations by Chelikowsky and Schluter (CS). The major disagreements are that CS predict an indirect absorption edge, and their conduction bands are much wider than ours. Possible reasons for these disagreements are suggested.

I. INTRODUCTION

We have calculated the electronic energy bands of silicon dioxide in the α-, or low, quartz structure, a hexagonal lattice[1] with 3 silicons and 6 oxygens in the coordination unit. This is an extension of the recent work of Schneider and Fowler[2] on ideal β-cristobalite, a high-symmetry form of SiO_2. Pantelides and Harrison[3] and Ciraci and Batra[3] have reported similar results on β-cristobalite. It has been argued, with good reason,[2,3] that much of the physics extracted from these results can be applied to other forms of SiO_2, even in the amorphous state. The present calculations, on a real form of SiO_2 which exhibits bending of the Si-O-Si bond, were performed to test this proposition and at the same time to provide information about the most common and important crystalline form of SiO_2, α-quartz.

These calculations were performed using the generalized mixed-basis method[4,5] in much the same fashion[2] as recently reported for β-cristobalite, and for this reason little is said about the method or the details of the calculations. Considerable effort was given to developing the group theory of α-quartz[6] into a form suitable for computation, based upon the earlier work of Frei.[7]

The results of these calculations provide a basis for a consistent interpretation of a variety of experiments. Comparisons with results on β-cristobalite indicate that long-range effects only slightly influence the spectral properties of SiO_2. Subsequent to the completion of this work, Schluter and Chelikowsky[8] reported the results of pseudopotential calculations of the α-quartz energy bands. Their results are discussed and compared with ours.

II. CALCULATIONS

A. Crystal structure and symmetry properties

α-quartz is a form of SiO_2 which is stable at room temperature. It exists in both right- and left-handed forms, to which correspond two enantiomorphous space groups, $D_3^6 = P3_221$ and $D_3^4 = P3_121$, respectively.[1] Although both forms often coexist in real crystals, we have considered only the right-handed form (D_3^6).

The Bravais lattice is hexagonal Γ_h. The orthogonal components of the three primitive translation vectors are

$$\begin{aligned} \vec{t}_1 &= a(\sqrt{3}/2, -\tfrac{1}{2}, 0), \\ \vec{t}_2 &= a(0, 1, 0), \\ \vec{t}_3 &= c(0, 0, 1), \end{aligned} \tag{1}$$

where $a = 9.282$ Bohr radii, and $c/a = 1.0986$.[9] The vector $\vec{t}_3$ is directed along the z axis and has length c; the vectors $\vec{t}_1$ and $\vec{t}_2$, both of length a, lie in the x-y plane and form an angle of $\frac{2}{3}\pi$ with each other.

The primitive cell contains 9 atoms, 3 Si and 6 O. Each silicon has 4 oxygen neighbors in an approximately tetrahedral arrangement, while each oxygen has 2 silicon neighbors with a Si-O-Si angle of approximately 144°. The positions of these 9 atoms are given in Table I, in terms of the primitive vectors (hexagonal coordinates).

The primitive vectors of the reciprocal lattice are

$$\begin{aligned} \vec{g}_1 &= (2\pi/a)(2/\sqrt{3}, 0, 0), \\ \vec{g}_2 &= (2\pi/a)(1/\sqrt{3}, 1, 0), \\ \vec{g}_3 &= (2\pi/c)(0, 0, 1). \end{aligned} \tag{2}$$

TABLE I. Hexagonal coordinates of atoms in the primitive cell of right-handed α-quartz. Here $k=0.465$, $l=0.415$, $m=0.272$, $n=0.120$, $\tau=\frac{1}{3}$.

Coefficients of:		$\vec{t}_1$	$\vec{t}_2$	$\vec{t}_3$
Si	1	k	0	0
	2	$1-k$	$1-k$	τ
	3	0	k	2τ
O	1	l	m	n
	2	$1-l$	$1-l+m$	$-n+\tau$
	3	$1-l+m$	$1-l$	$n+\tau$
	4	$l-m$	$1-m$	$1-n$
	5	$1-m$	$l-m$	$n+2\tau$
	6	m	l	$-n+2\tau$

The Brillouin zone (BZ) is shown[6,7] in Fig. 1. Points of high symmetry are indicated on the figure and are defined in the caption. In order to obtain the irreducible representations (Ir. rep.) of the space group corresponding to a given point of symmetry $\vec{k}$ in the BZ, we used Herring's[10] method (Ref. 6, pp. 167, 168). This involves the Ir. rep. of the factor group $G^{\vec{k}}/T^{\vec{k}}$, where $G^{\vec{k}}$ is the little group of $\vec{k}$ and $T^{\vec{k}}$ is the group of all translations $\vec{t}$ which satisfy the condition

$$\exp(-i\vec{k}\cdot\vec{t})=1\,. \tag{3}$$

Those Ir. rep. of the factor group which, for an arbitrary translation $\{E|\vec{t}\}$, satisfy the condition

$$\Gamma(\{E|\vec{t}\})=\exp(-i\vec{k}\cdot\vec{t})\underline{1}\,, \tag{4}$$

where $\underline{1}$ is the unit matrix, yield Ir. rep. for the space group.

We performed calculations for the points Γ, A, K, and H in the BZ. For Γ, the factor group G^{Γ}/T^{Γ} is isomorphic to the point group D_3 and is thus of order 6. For each of the other cases the factor group is of larger order but may be written as the direct product of a group of order 6, isomorphic to D_3, times one or more groups of order 2 or 3. As discussed in Sec. II B, this means that for each case the little co-group of the $\vec{k}$ vector is of order 6, and comparable accuracy of the energy eigenvalues at each of these points may be obtained. Other points of interest, such as M, are of lower symmetry and have not been treated in the present calculations.

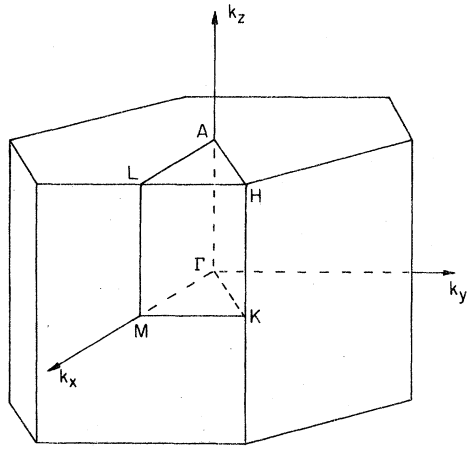

FIG. 1. Brillouin zone for Γ_h. In terms of the directions k_x, k_y, k_z, $\Gamma=(0,0,0)$, $A=(2\pi/a)\ (0,0,a/2c)$, $K=(2\pi/a)\ (1/\sqrt{3},\frac{1}{3},0)$, $H=(2\pi/a)\ (1/\sqrt{3},\frac{1}{3},a/2c)$, $M=(2\pi/a)\ (1/\sqrt{3},0,0)$, $L=(2\pi/a)\ (1/\sqrt{3},0,a/2c)$.

B. Mixed-basis calculation

The crystal potential was defined as in Ref. 2 as the sum of the free-atom neutral silicon and oxygen potentials obtained from the modified Herman-Skillman[11] computer codes. The exchange potentials were of the Slater $\rho^{1/3}$ type,[12] with coefficient (α) equal to 1. Other aspects of the mixed-basis calculation were also discussed in Ref. 2. Reference 2 also contains a discussion of the use of free-atom versus ionic potentials as well as other possible sources of error in the calculations.

The basis functions were of two types[2,4,5]; Bloch sums, from symmetrized combinations of atomic-like orbitals (SCAO), and symmetrized combinations of plane waves (SCPW). Apart from a normalization factor, the two types of functions have the form

$$\psi(\mathrm{SCAO})=\sum_{\{R|\vec{v}\}}\Gamma^{*}_{11}(\{R|\vec{v}\})\times e^{-i\vec{k}\cdot\vec{t}'}\phi_{\mu'\rho}[R^{-1}(\vec{r}-\vec{d}_{\mu'})]\,, \tag{5}$$

$$\psi(\mathrm{SCPW})=\sum_{\{R|\vec{v}\}}\Gamma^{*}_{11}(\{R|\vec{v}\})\times e^{-iR(\vec{k}+\vec{h}_j)\cdot\vec{v}}e^{iR(\vec{k}+\vec{h}_j)\cdot\vec{r}}\,. \tag{6}$$

In both equations, $\sum_{\{R|\vec{v}\}}$ is a sum over all coset representatives of the factor group $G^{\vec{k}}/T^{\vec{k}}$, and $\Gamma^{*}_{11}(\{R|\vec{v}\})$ is the complex conjugate of the element 11 of the matrix of the Ir. Rep. which corresponds to the element $\{R|\vec{v}\}$. $\vec{t}'$ is a lattice translation defined by

$$\{R|\vec{v}\}\,\vec{d}_{\mu}=\vec{d}_{\mu'}+\vec{t}'\,, \tag{7}$$

where $\vec{d}_{\mu}$ and $\vec{d}_{\mu'}$ are position vectors of equivalent atoms in the primitive cell, and $\phi_{\mu'\rho}[R^{-1}(\vec{r}-\vec{d}_{\mu'})]$ is an atomic-like orbital centered on the atom at $\vec{d}_{\mu'}$. $\vec{h}_j$ is a reciprocal-lattice vector. $\psi(\mathrm{SCPW})$ is of the form which enters the MB expansion, while if $\psi(\mathrm{SCAO})$ is called $\psi(\vec{r})$, the function which enters the MB expansion is $\sum_{\vec{t}}\exp(i\vec{k}\cdot\vec{t})\,\psi(\vec{r}-\vec{t})$.

In those cases where the group $G^{\vec{k}}/T^{\vec{k}}$ can be written as a direct product $G_6\otimes T_n$, the sum over

$\{R|\vec{v}\}\in G^{\vec{k}}/T^{\vec{k}}$ can be written as a double sum, one over the elements $\{R|\vec{\omega}\}\in G_6$ and the other over the translations $\{E|\vec{t}_i\}\in T_n$. The latter sum contributes a constant factor and can be neglected. Thus, the sums in Eqs. (5) and (6) can be restricted to the coset representatives of the group G_6.

III. ENERGY BANDS

A. General

Figures 2 and 3 show the computed valence and conduction bands, respectively. The computed energies are indicated by shaded circles. These points are connected by smooth curves which were drawn so as to satisfy compatibility relations[7] and to intersect points of high symmetry with proper slopes.[13]

The open circles in Fig. 3 indicate the intersection of a free-electron energy band plotted on the same scale as the bottom of the conduction band which passes through Γ_1. This Γ_1 has for convenience been chosen as the zero of energy.

The accuracy of these results was optimized by including many plane waves in the basis, leading to 98×98 matrices for Γ_3, A_3, K_3, and H_3, and by studying the relative convergence (energy versus number of basis functions) of the solutions. It appears that the convergence obtained here was comparable to that obtained for β-cristobalite[2] (~0.05 to 0.2 eV) and was therefore not a significant source of error.

In order to assess the atomic character of the wave functions, a projection technique developed earlier by the authors[5] was used. The quantity Q^{σ}_{pn} was obtained, defined by

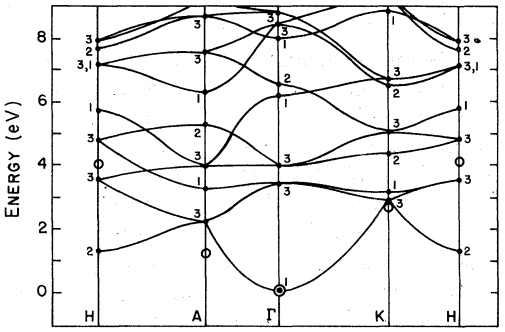

FIG. 3. Lowest conduction bands of α-quartz. Computed points are indicated by dots. Open circles at A, H, and K indicate where free-electron bands would intersect these points. The zero of energy is defined as the bottom of the conduction band.

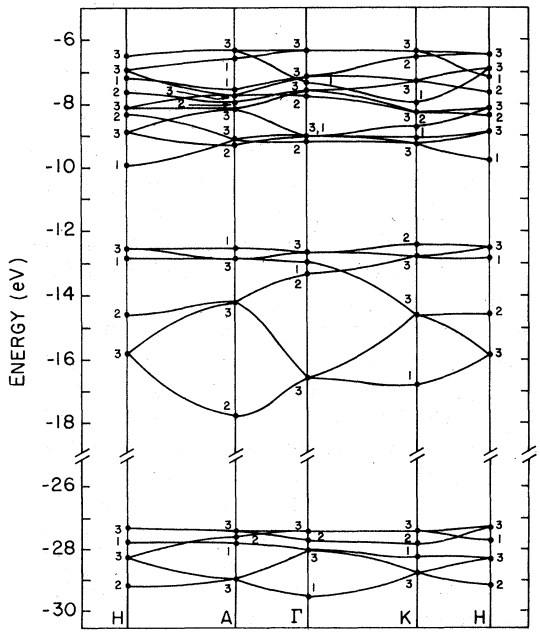

FIG. 2. Valence bands of α-quartz. Computed points are indicated by dots. The energy scale is defined so that the bottom of the conduction band is at zero. In units of $2\pi/a$, Γ is $(0,0,0)$, A is $(0,0,1/2.2)$, K is $(1/\sqrt{3},\frac{1}{3},0)$, and H is $(1/\sqrt{3},\frac{1}{3},1/2.2)$. Note the break in the vertical scale.

TABLE II. Projection results for symmetrized tight-binding Bloch sums built up from nonoverlapping atomic-like s and p orbitals at the point Γ. In each case the quantity Q^{σ}_{pn}, defined in Eq. (8), is tabulated.

Band composition	Ir. rep. at Γ	Si $3s$	Si $3p$	O $2s$	O $2p$
Oxygen	Γ_1	4		57	
$2s$ valence band	Γ_3	1	1	63	
	Γ_2		1	66	
	Γ_3		1	67	
Si-O covalent	Γ_3	11	1	2	30
bonding bands	Γ_2		7		41
	Γ_1		7		44
	Γ_3		7		41
Oxygen $p\pi$	Γ_2		3	3	45
lone-pair bands	Γ_1	2		5	46
	Γ_3		1	2	46
	Γ_2				57
	Γ_3				56
	Γ_1	2		2	56
	Γ_3		1	2	54
	Γ_3				60
Lower	Γ_1	14		19	9
conduction bands	Γ_3	1	13	6	5
	Γ_3	2	11	7	10
	Γ_1	5	2		5
	Γ_2		10	4	24

$$Q^{\sigma}_{pn} = 100 |\langle F^{\sigma}_{p} | \psi^{\sigma}_{n} \rangle|^2 , \quad (8)$$

where σ is the irreducible representation, n labels the total wave function ψ^{σ}_{n}, and p labels the Bloch function F^{σ}_{p}. Q^{σ}_{pn} then gives the percent contribution of the Bloch function F^{σ}_{p} to the total wave function ψ^{σ}_{n}. Table II gives these results for those symmetry allowed silicon 3*s* and 3*p* and oxygen 2*s* and 2*p* Bloch sums used in the basis at Γ. While these provide useful guidance, it should be noted that cutoff orbitals[14] have been used in the Bloch sums, a fact which will have some effect on the projection results.

B. Valence bands

The computed valence-band energies are indicated in Fig. 2, and the wave-function coefficients at the point Γ are given in Table II. In order to obtain information about the bands at general points in the BZ, we used a tight-binding interpolation scheme[15] identical in concept to that applied to β-cristobalite.[2] In this scheme, only oxygen *s* orbitals were used for the bands from ~−27 to −30 eV, while only oxygen *p* orbitals were used for the bands from ~−6 to −18 eV. The actual positions of the oxygen atoms were used in writing the phase factors of the Bloch functions, but the small differences in oxygen-oxygen separation were ignored in parametrizing the overlap integrals occurring in the calculations.

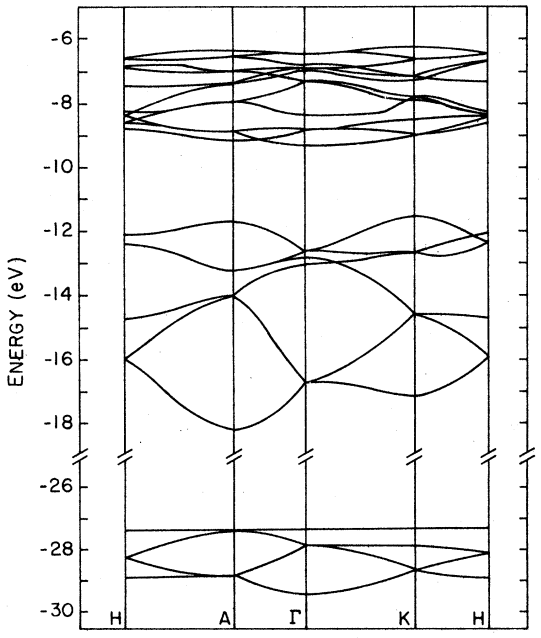

FIG. 4. Valence bands of α-quartz. These were obtained by a tight-binding fitting procedure discussed in the text. Note the break in the vertical scale.

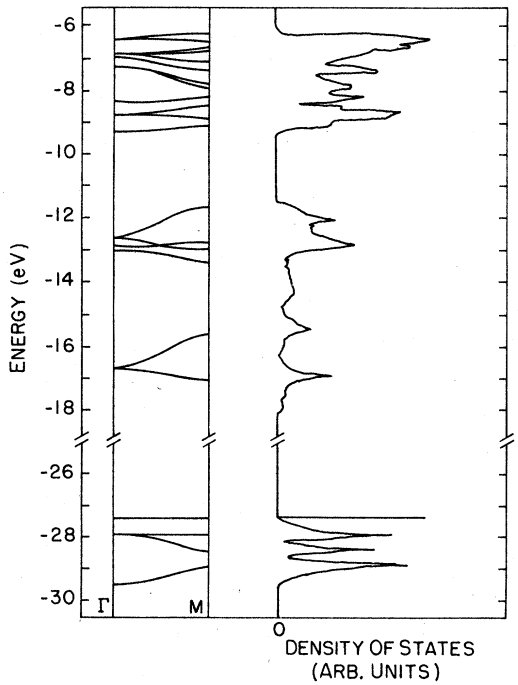

FIG. 5. Left panel: Valence bands of α-quartz from Γ to *M*. Right panel: Density of states in the valence bands of α-quartz. These curves were obtained by a tight-binding fitting procedure discussed in the text. Note the break in the vertical scale.

For the *s* bands there are two parameters, one which locates the centroid of the bands and a second which determines their widths. A 6×6 matrix was diagonalized to obtain the energies. For the *p* bands there is a centroid and a width parameter, and in addition a third parameter which determines the separation of the lone-pair and bonding bands. Only σ-type overlaps were considered. In this case an 18×18 matrix was diagonalized.

Figures 4 and 5 show tight-binding bands in which the parameters have been chosen to give good agreement with the computed bands at the point Γ. The overall agreement seems satisfactory. The major differences include the following: (i) The top of the computed valence band is rather flat, with a maximum at Γ. The corresponding tight-binding band is not as flat and the energy at the point *K* is ~0.14 eV higher than that at Γ. (ii) The computed Si-O bonding bands are flatter than those obtained from the tight-binding fit. (iii) Accidental degeneracies appearing in the upper part of the tight-binding 2*s* bands are not present in the computed bands.

Figure 5 shows tight-binding bands from Γ to *M*; the latter point was not obtained in the computer calculations. Also shown is a computed density-

of-states histogram obtained from the tight-binding valence bands. Energies were computed for up to 500 k values in $\frac{1}{24}$ of the BZ. By varying the mesh size and the plotting grid it was established that the prominent peaks are genuine. It is interesting to note that most of the peaks correspond to energies at M. In this sense, M is analogous to the point L in β-cristobalite.[2]

From Table II it can be seen that the lowest valence bands are predominantly derived from oxygen $2s$. The relatively small amounts of silicon $3s$ and $3p$ are concentrated in the lower and upper parts of the bands, respectively. The next set of bands (the Si-O covalent bonding bands) are oxygen-$2p$-rich but contain significant amounts of silicon $3s$ and $3p$, again concentrated in the lower ($3s$) and upper ($3p$) parts of the bands. The highest valence bands are mostly from oxygen $2p$ with small amounts of O $2s$ and Si $3s$ and $3p$.

C. Conduction bands

The lowest conduction-band minimum is at Γ_1. Free-electron energies at the points A, K, and H are indicated by circles in Fig. 3. The effective mass at Γ_1 is expected to be anisotropic, but we have not computed its value.

The lower conduction bands contain considerable admixtures of Si $3s$ and $3p$ and O $2s$ and $2p$ orbitals. These are the antibonding counterparts to the bonding valence bands. Their topology, however, resembles more closely that of the oxygen $2s$ bands; in particular, the band shape near the lowest H point (H_2) is not at all free-electron-like but is similar to the shape near H_2 in the $2s$ bands. This suggests that oxygen s components play a significant role in the lowest conduction bands.[8] Other remarks about the conduction bands are to be found in Sec. IV.

IV. COMPARISONS WITH OTHER CALCULATIONS AND WITH EXPERIMENT

In the following discussion the present results on α-quartz are compared with various experiments and also with calculations on β-cristobalite by Schneider and Fowler[2] and on α-quartz by Chelikowsky and Schluter (CS).[8]

A. Band gap and absorption edge

The computed band gap is direct at the point Γ, with magnitude 6.3 eV. This is close to the 6.0 eV obtained for β-cristobalite,[2] but both values are less than 8.9 eV obtained from photoconductivity measurements[16] and 9.2 eV computed[8] by CS. It is not uncommon for calculations employing the $\rho^{1/3}$ exchange as used here to underestimate the band gap[17] even while giving bands of reasonable structure. As discussed in Sec. V, a better treatment of exchange might well yield a better value of the gap.

The absorption edge is Γ_3 to Γ_1, which is allowed by symmetry. This could, in principle, represent an important difference from the edge in β-cristobalite, which was predicted to be direct forbidden.[2] In order to investigate this further, we estimated the relative strengths of transitions to the Γ_1 conduction-band minimum from the 4 Γ_3 states and the 2 Γ_2 states in the upper valence bands. This was done by treating the Γ_1 final state as a linear combination of oxygen s orbitals and considering only one-center terms in the electric dipole matrix elements between the s orbital and the oxygen p orbitals contained in the valence wave functions. While this may not give quantitatively accurate results, it does allow symmetry effects in the valence states to be exhibited.

The results of this estimate are striking. On a scale in which the strongest transition has magnitude 1, the strengths from the upper two Γ_3 states are less than 10^{-3}. That from the third Γ_3 state (at -7.7 eV on the energy scale of Fig. 2) is 1, and that from the fourth Γ_3 state is less than 10^{-3}. The strength from the Γ_2 state at -7.9 eV is 0.95, and that from the lower Γ_2 state is less than 6%. Thus, the preponderance of the oscillator strength at Γ arises from states ~1.5 eV below the top of the valence band.

In view of this situation, it seems necessary to regard the predicted absorption band edge in α-quartz to be direct forbidden, to a high degree of approximation. The rigorous selection rule in β-cristobalite is only slightly relaxed in α-quartz, and appears to be mostly related to short-range order in SiO_2. It is logical to expect a similar approximate selection rule in amorphous SiO_2.

As discussed in Ref. 2, a direct forbidden absorption edge has no $n=1$ exciton associated with it,[18] and such experimentally[19,20] appears to be the case in both α-quartz and amorphous SiO_2; that is, there is no strong exciton peak at an energy *lower* than 8.9 eV.

Chelikowsky and Schluter[8] have predicted an *indirect* band gap of 9.2 eV, due to upward bending of the valence bands away from Γ. The direct gap at Γ is ~9.7 eV, which is stated to be forbidden. Both these numbers are closer to experiment than obtained here. Of greater note, however, is their prediction of an indirect edge, in disagreement with our results. It is interesting to note that our tight-binding valence bands *do* have maxima away from Γ, but only by ~0.14 eV. This feature probably arises from the small basis set used in the tight-binding fit: the oxygen p orbitals mix and

their energies are pushed apart, and there are no higher orbitals (e.g., Si 3s and 3p) to mix and push these energies down again. In silver and alkali halides such effects have produced spurious maxima along [100] directions,[21] at Δ_1. The question of a direct forbidden versus an indirect edge can be settled experimentally, but it appears that such detailed low-temperature spectroscopy has not yet been done on SiO_2.

B. Silicon and oxygen x-ray emission spectra

These spectra, and the photoemission spectra discussed in Sec. IV C, probe the nature of the valence bands, and before we make comparisons of theory versus experiment some remarks about our computed valence bands as compared to those of CS and the valence bands of β-cristobalite are in order.

Overall, the present valence bands and those computed by CS are in quite good agreement. Our lone-pair and bonding bands are ~1 eV narrower than theirs, and as mentioned above they predict valence-band maxima away from Γ. However, superposition of our computed tight-binding density of states with theirs reveals good agreement of the locations of the maxima in the lone-pair and bonding bands. Their oxygen 2s band appears to be somewhat narrower than ours; their 2s bands are ~5 eV too low, ours ~2.5 eV too low with respect to experiment.

As compared with β-cristobalite,[2] the present 2s and bonding bands are comparable in width. The present oxygen lone-pair bands are ~2 eV wider.

Figure 6 shows a comparison of computed (and adjusted) tight-binding densities of states (DOS) with experimental x-ray emission spectra.[22,23] In order to obtain reasonable agreement with experiment, the lone pair DOS were shifted down by ~1 eV and the oxygen-2s DOS were shifted up by ~1.5 eV. A lengthy discussion of these spectra and their interpretation is contained in Ref. 2 and will not be repeated here. It is sufficient to point out here that the experimental peaks (indicated by arrows) agree fairly well with computed DOS peaks, and that the atomic nature of the valence-band wave functions is consistent with these peaks, as was also the case for β-cristobalite.

The above statement, however, must be qualified in one respect. The highest Si $L_{2,3}$ peak must originate from either Si s or d wave-function admixture into the lone-pair bands. The amount of 3s computed for this region is not sufficient to account for such a strong peak, and it was concluded in Ref. 2 that this peak represented the effect of Si-3d admixture into these bands. Such an orbital was not included in our wave-function basis, so we have not computed a value for this admixture. It was pointed out[2] that this admixture could be small in absolute terms and still be important in SiO_2 chemistry, as has been suggested.[24]

Chelikowsky and Schluter have computed the x-ray emission spectra for α-quartz,[8] by calculating transition probabilities from their orthogonalized valence-band wave functions to the core states. They obtained very good agreement with experiment, with the exception that their highest Si $L_{2,3}$ peak was much too weak. They argued that this reflects a relatively small amount of Si-3d-like wave function in the valence bands, and suggested that the experimental results may be faulty and that the peak in question may arise from elemental silicon created by the electron beam.

This criticism of the experiments of Wiech, however, does not seem well founded in view of his description[25] of the procedures taken to investigate and avoid this spurious effect. The absence of sufficient Si-3d orbital in the valence states of CS must then be considered; this may be associated with the fact that they did not include any $l=2$ terms in the pseudopotential.

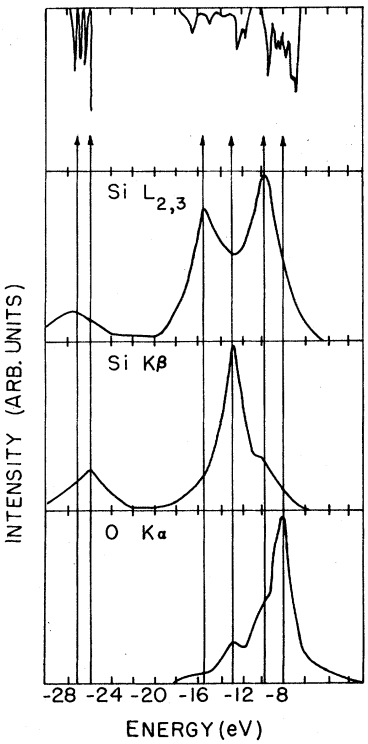

FIG. 6. Comparison of experimental x-ray emission spectra with a density of states obtained from the tight-binding valence bands, and shifted in energy. The vertical lines terminated by arrowheads pass through peaks in the experimental curves. The energy scale is that used in Ref. 2 (see text and Ref. 22 for details).

C. Photoemission results

Ultraviolet (UPS) and x-ray (XPS) photoemission spectra were obtained several years ago by DiStefano and Eastman.[26] Since that time several other spectra have appeared, all in general agreement with those of Ref. 26. The spectra of Nagel *et al.*[27] and Stephenson and Binkowski[28] on various forms of SiO_2 have noted the dependence of a low-energy tail on the nature of the sample. Although Stephenson and Binkowski[28] argued that this tail is an intrinsic feature, implications of this do not seem tenable, as discussed in Ref. 2, and the DiStefano-Eastman spectra still seem to represent intrinsic SiO_2. Because these spectra are generally consistent with x-ray emission data and have been discussed in Ref. 2, they are not discussed further here.

D. Optical-reflectivity data

The optical-reflectivity data of Refs. 19 and 20 cover a region of ~10 eV above the band gap and thus provide potential information on both conduction and valence bands. These data consist of peaks at ~10.3, 12.0, 14.4, and 17.2 eV in both α-quartz and amorphous SiO_2. Platzöder[20] has barely resolved the 12.0-eV peak into 3 components and has noted that the 10.3-eV peak has an asymmetric shape characteristic of a Fano resonance[29]; he suggested that it may be a metastable exciton.[30]

Chelikowsky and Schluter have computed[6] the interband absorption spectra from their α-quartz bands. After shifting the theoretical spectrum up by 0.7 eV they found peaks at ~11.7 and 14.0 eV, in approximate agreement with the second and third experimental peaks (although their relative absorption strengths agreed very poorly with experiment). They then argued that the 10.3 eV peak is due to an exciton.

Since these data probe both valence and conduction bands, it is worthwhile here to compare our conduction bands with those of CS. We find that although the shapes of the lower conduction bands are in fair agreement, there is serious disagreement with respect to bandwidths. For example, the separation of the first two states at Γ was computed by CS to be ~6 eV, while we find it to be 3.4 eV. Similar differences were found at K, H, and A, the smallest difference being ~1 eV at A. Their conduction bands, then, are much wider than ours, a fact consistent with the small electron effective mass ($0.3m_e$) which they obtained.

The wide conduction bands of CS are critical to their interpretation of the optical spectra; this tends to mean that structure in the spectrum must originate from lower valence bands. In our case, there is also the possibility of transitions from the highest valence bands into the next conduction bands. Since we have not computed interband transition strengths we simply mention some possible assignments for the peaks, in much the same way as was done for β-cristobalite.[2]

First, as discussed above, the band edge is direct forbidden and occurs, presumably at ~8.9 eV. A direct allowed edge will occur between the Γ_3 and Γ_2 valence states ~1.3 eV below the top of the band, and the lowest Γ_1; this occurs at 10.2 eV. Such bands might be expected to generate a fairly predominant exciton, but if that exciton is the absorption peak at 10.3 eV, then the Γ_3-Γ_2 pair should be ~0.5 eV lower in the valence band than we have computed. As noted by Platzöder, such an exciton is indeed degenerate with continuum states.

A second possible source of strong interband transition strength could be from states at M, where joint densities of states are large. Since the free-electron energy at M is 2.1 eV, one might expect a strong peak ~2 eV above Γ_1, possibly exciton-enhanced and shifted to lower energies. A similar assignment was made at the point L in β-cristobalite.

Further detailed assignments of transitions appear difficult, in view of our lack of knowledge of the conduction bands at the point M; however, it seems evident that the many conduction bands between 0 and 4 eV lead to various possibilities.

V. DISCUSSION AND CONCLUSIONS

Reference 2 contains a discussion of possible errors in the type of calculation reported here. In that paper it was argued that the use of atomic rather than ionic potentials was likely to be much less serious than one would initially suppose, since the Madelung field in which each ion finds itself tends to neutralize the charge on the ion.

More serious, we feel, is our treatment of exchange as a sum of atomic $\rho^{1/3}$ terms rather than summing ρ and then taking the $\frac{1}{3}$ power. We intend to carry out further calculations in which exchange potentials closer to the correct form are used. Since there is no simple systematic way of doing this, we choose the simplest approximation for the present calculations.

The exchange potential which we have used is too large in the region in which atomic charge densities overlap, i.e., the system behaves as if it has too much charge (or too large a potential) between the atoms. The effect of this approximation was investigated some time ago in connection with a tight-binding calculation of the valence bands of krypton,[31] and an interesting result emerged: the (poorer) atomic $\rho^{1/3}$ exchange pushed s and p valence bands apart. This occurred because σ-type

two-center potential energy s integrals were affected more than corresponding p integrals by the extra potential between the atoms. This may be significant since in both β-cristobalite and α-quartz our computed oxygen $2s$ and $2p$ valence bands are too far apart, by ~2–2.5 eV. We believe that a better exchange potential will bring these bands into better agreement with experiment.

It should be noted here that CS's oxygen $2p$ and $2s$ bands were computed to be too far apart by 5 eV. This is a large discrepancy which in the light of the above discussion suggests that their calculation bears further investigation.

In the krypton calculations mentioned above, improving the exchange potential also led to a larger (and better) gap between valence and conduction bands. We speculate that the same may occur here.

It is difficult to assess CS's prediction of a valence-band maximum away from $\vec{k}=0$, and a consequent indirect absorption edge, as opposed to our prediction of a maximum at $\vec{k}=0$ with a direct (and forbidden) absorption edge. To our knowledge no experiments have been performed which bear upon this question in SiO_2; however, a careful optical study[32] of GeO_2 (tetragonal structure) indicates a direct forbidden absorption edge, and the same appears to be true for SnO_2. On the theoretical side, we found a maximum away from $\vec{k}=0$ to occur in a simple tight-binding fit of the valence bands; we argued that this was a spurious result, most likely arising from the small wave-function basis used in the fit. However, because CS's method of calculation is so different from ours, we cannot determine the origin of their maximum away from $\vec{k}=0$.

An additional point of comparison concerns the conduction-band structure, with CS's bands being wider than ours. Again, it is difficult to conclude which result is better. In favor of our result is the fact that similar conduction bands were obtained for β-cristobalite using two independent methods, the mixed-basis calculation of Ref. 2 and an extended-tight-binding calculation by Ciraci and Batra[3] using Gaussian-type orbitals.

It is finally to be noted that our calculations indicate that α-quartz shares many physical properties with ideal β-cristobalite. In particular, the top of the valence band is rather flat and the optical-absorption edge is direct forbidden. Densities of states in the valence bands are similar, as are the wave-function admixtures in various parts of the bands. These similarities in turn strongly suggest that amorphous SiO_2 should have many of the same properties as the crystalline forms, as indeed seems to be the case.

ACKNOWLEDGMENTS

The authors express their appreciation to Dr. Philip M. Schneider for his important assistance in the computational parts of this problem. Professor Frank Feigl of Lehigh contributed much help and encouragement. The help of the computing centers at Lehigh and at Brookhaven National Laboratory is also gratefully acknowledged. Some of the calculations were done using the facilities of the CINECA, through the terminal at the computing center of the University of Parma. This research was supported in part by the NSF, Grant No. DMR 71-01798 A02.

[1]H. D. Megaw, *Crystal Structures: A Working Approach* (Saunders, Philadelphia, 1973); R. W. G. Wyckoff, *Crystal Structures*, 2nd ed. (Interscience, New York, 1963), Vol. 1.

[2]Philip M. Schneider and W. Beall Fowler, Phys. Rev. Lett. 36, 425 (1976); Philip M. Schneider and W. Beall Fowler, Phys. Rev. B (to be published).

[3]S. T. Pantelides and W. A. Harrison, Phys. Rev. B 13, 2667 (1976); S. Ciraci and I. P. Batra, Phys. Rev. B 15, 4923 (1977).

[4]A. B. Kunz, Phys. Rev. 180, 934 (1969).

[5]E. Calabrese and W. B. Fowler, Phys. Status Solidi B 56, 621 (1973).

[6]C. J. Bradley and A. P. Cracknell, *The Mathematical Theory of Symmetry in Solids* (Oxford University, 1972).

[7]V. Frei, Czech. J. Phys. B 17, 147 (1967); 233 (1967).

[8]M. Schluter and J. R. Chelikowsky, Solid State Commun. 21, 381 (1977); J. R. Chelikowsky and M. Schluter, Phys. Rev. B 15, 4020 (1977).

[9]*Crystal Data, Determinative Tables, 3rd ed., Vol. 2: Inorganic Compounds*, edited by J. D. H. Donnay and H. M. Ondik (U.S. Dept. of Commerce, Springfield, Va., 1973).

[10]C. Herring, J. Franklin Inst. 233, 525 (1942).

[11]F. Herman and S. Skillman, *Atomic Structure Calculations* (Prentice-Hall, Englewood Cliffs, N.J., 1963).

[12]J. C. Slater, Phys. Rev. 81, 385 (1951).

[13]C. Herring, Phys. Rev. 52, 361 (1937); 365 (1937).

[14]R. A. Deegan and W. D. Twose, Phys. Rev. 164, 993 (1967).

[15]J. C. Slater and G. F. Koster, Phys. Rev. 94, 1498 (1954).

[16]T. H. DiStefano and D. E. Eastman, Solid State Commun. 9, 2259 (1971).

[17]N. O. Lipari and W. B. Fowler, Phys. Rev. B 2, 3354 (1970).

[18]R. J. Elliott, Phys. Rev. 108, 1384 (1957).

[19]H. R. Philipp, J. Phys. Chem. Solids 32, 1935 (1971).

[20]K. Platzöder, Phys. Status Solidi 29, K63 (1968).

[21]F. Bassani, R. S. Knox, and W. B. Fowler, Phys. Rev. 137, A1217 (1965); A. B. Kunz, Phys. Rev. 151, 620 (1966).

[22]The silicon $L_{2,3}$ and $K\beta$ spectra are reported by G. Wiech, in *Soft X-Ray Band Spectra*, edited by D. J. Fabian (Academic, New York, 1968). The oxygen $K\alpha$ spectrum is from G. Klein and H.-U. Chun, Phys. Status Solidi B 49, 167 (1962). The relative positions of oxygen and silicon spectra are after R. A. Pollak (private communication), but the assignment of the valence-band edge is ours. See also B. Fischer, R. A. Pollak, T. H. DiStefano, and W. D. Grobman, Phys. Rev. B 15, 3193 (1977).

[23]These and other data and their analysis are discussed in a review article by D. Griscom, J. Non-cryst. Solids 24, 155 (1977).

[24]A. G. Revesz, J. Non-cryst. solids 4, 347 (1970); Phys. Rev. Lett. 27, 1578 (1971).

[25]G. Wiech, Z. Phys. 207, 428 (1967).

[26]T. H. DiStefano and D. E. Eastman, Solid State Commun. 9. 2259 (1971).

[27]S. R. Nagel, J. Tauc, and B. G. Bagley, Solid State Commun. 20, 245 (1976).

[28]D. A. Stephenson and N. J. Binkowski, J. Non-cryst. Solids 22, 399 (1976).

[29]U. Fano, Phys. Rev. 124, 1866 (1961).

[30]K. P. Jain, Phys. Rev. 139, A544 (1965).

[31]W. B. Fowler, Phys. Rev. 132, 1591 (1963).

[32]M. Stapelbroek and B. D. Evans, Solid State Commun. (to be published).